

# UC Irvine

## UC Irvine Previously Published Works

### Title

Single-channel characteristics of wild-type IKs channels and channels formed with two minK mutants that cause long QT syndrome.

### Permalink

<https://escholarship.org/uc/item/8nr0s1s3>

### Journal

The Journal of general physiology, 112(6)

### ISSN

0022-1295

### Authors

Sesti, F  
Goldstein, SA

### Publication Date

1998-12-01

### DOI

10.1085/jgp.112.6.651

### Copyright Information

This work is made available under the terms of a Creative Commons Attribution License, available at <https://creativecommons.org/licenses/by/4.0/>

Peer reviewed

# Single-Channel Characteristics of Wild-Type $I_{Ks}$ Channels and Channels formed with Two MinK Mutants that Cause Long QT Syndrome

FEDERICO SESTI and STEVE A.N. GOLDSTEIN

From the Section of Developmental Biology and Biophysics, Departments of Pediatrics and Cellular and Molecular Physiology, Boyer Center for Molecular Medicine, Yale University School of Medicine, New Haven, Connecticut 06536-0812

**ABSTRACT**  $I_{Ks}$  channels are voltage dependent and  $K^+$  selective. They influence cardiac action potential duration through their contribution to myocyte repolarization. Assembled from minK and KvLQT1 subunits,  $I_{Ks}$  channels are notable for a heteromeric ion conduction pathway in which both subunit types contribute to pore formation. This study was undertaken to assess the effects of minK on pore function. We first characterized the properties of wild-type human  $I_{Ks}$  channels and channels formed only of KvLQT1 subunits. Channels were expressed in *Xenopus laevis* oocytes or Chinese hamster ovary cells and currents recorded in excised membrane patches or whole-cell mode. Unitary conductance estimates were dependent on bandwidth due to rapid channel "flicker." At 25 kHz in symmetrical 100-mM KCl, the single-channel conductance of  $I_{Ks}$  channels was  $\sim 16$  pS (corresponding to  $\sim 0.8$  pA at 50 mV) as judged by noise-variance analysis; this was fourfold greater than the estimated conductance of homomeric KvLQT1 channels. Mutant  $I_{Ks}$  channels formed with D76N and S74L minK subunits are associated with long QT syndrome. When compared with wild type, mutant channels showed lower unitary currents and diminished open probabilities with only minor changes in ion permeabilities. Apparently, the mutations altered single-channel currents at a site in the pore distinct from the ion selectivity apparatus. Patients carrying these mutant *minK* genes are expected to manifest decreased  $K^+$  flux through  $I_{Ks}$  channels due to lowered single-channel conductance and altered gating.

**KEY WORDS:** KvLQT1 • heart • potassium • long QT syndrome • delayed rectifier

## INTRODUCTION

Two voltage-dependent  $K^+$  currents,  $I_{Ks}$  and  $I_{Kr}$ , bring the heart beat to an end by repolarization of the myocardium (Sanguinetti and Jurkiewicz, 1990, 1991). The  $K^+$  channel mediating  $I_{Ks}$  is formed by coassembly of two gene products, KvLQT1 and minK (Barhanin et al., 1996; Sanguinetti et al., 1996b). KvLQT1 is a 581 residue protein with six transmembrane segments and a classical pore-forming P domain (Wang et al., 1996b); human minK has just 129 residues and one transmembrane segment (Takumi et al., 1988). While many  $K^+$ -selective pores are known to form by symmetrical alignment of four P loops around a central pathway (MacKinnon, 1991; Shen et al., 1994; Glowatzki et al., 1995; Doyle et al., 1998), the  $I_{Ks}$  channel pore incorporates minK residues, a non-P loop protein (Goldstein and Miller, 1991; Wang et al., 1996a; Tai and Goldstein, 1998). Six sites in the transmembrane stretch of minK are exposed in the  $I_{Ks}$  conduction pathway; two adja-

cent residues flank that portion of the pore that restricts transmembrane movement of  $Na^+$ ,  $Cd^{2+}$ , and  $Zn^{2+}$  ions; thus, position F55 is in contact with the external solution while G56 is accessible only to the cytosol (Tai and Goldstein, 1998). To delineate the attributes of this unique type of heteromeric ion conduction pathway, we sought to study  $I_{Ks}$  channels formed with wild-type and mutant minK subunits at the single-channel level.

Long QT syndrome (LQTS)<sup>1</sup> is characterized by an abnormally long interval between the QRS complex (reflecting ventricular depolarization) and the T wave (resulting from ventricular repolarization) on the surface electrocardiogram; thus, a long QT interval indicates prolongation of the cardiac action potential. Through an unknown mechanism, this predisposes the myocardium to an arrhythmia called torsade de pointes that can degenerate to ventricular fibrillation and sudden death (Dumaine et al., 1996; Keating and Sanguinetti, 1996a; Roden et al., 1996; Ackerman, 1998). Mutations in cardiac  $K^+$  channels that cause LQTS do so by decreasing  $K^+$  efflux from affected cells, thereby

Address correspondence to Steve A.N. Goldstein, Section of Developmental Biology and Biophysics, Departments of Pediatrics and Cellular and Molecular Physiology, Boyer Center for Molecular Medicine, Yale University School of Medicine, 295 Congress Avenue, New Haven, CT 06536-0812. Fax: 203-737-2290; E-mail: steve.goldstein@yale.edu

<sup>1</sup>Abbreviations used in this paper: CHO, Chinese hamster ovary; LQTS, long QT syndrome.

delaying repolarization (Sanguinetti et al., 1995, 1996a; Wang, et al., 1996b; Splawski et al., 1997). LQTS, first associated with mutations in *KvLQT1* and *HERG* K<sup>+</sup> channel genes has now been linked to mutations in the *minK* gene (Wang, et al., 1996b; Schulze-Bahr et al., 1997; Splawski, et al., 1997; Duggal et al., 1998). Inheritance of one mutant minK allele (encoding D76N or S74L minK) and one wild-type allele is associated with LQTS (Splawski, et al., 1997), while patients with two mutant alleles (S74L/D76N or D76N/D76N) present with LQTS and deafness (Schulze-Bahr et al., 1997; Duggal et al., 1998). Splawski et al. (1997) have shown that these mutations decrease K<sup>+</sup> currents by shifting activation of mutant I<sub>Ks</sub> channels to more depolarized potentials and by accelerating their deactivation.

Here we compare the properties of single channels formed with KvLQT1 subunits and those of I<sub>Ks</sub> channels containing human minK and KvLQT1 subunits. Thereafter, the effects of minK mutants on I<sub>Ks</sub> channel function are evaluated. Homomeric KvLQT1 channels are found to have a single-channel conductance fourfold lower than wild-type I<sub>Ks</sub> channels, in good agreement with a companion report by our colleagues (Yang and Sigworth, 1998), but in conflict with the findings of others (Romey et al., 1997). I<sub>Ks</sub> channels formed with minK mutants show lower unitary conductances than wild-type channels and, as previously detailed (Splawski et al., 1997), diminish open probability. Some implications of these results relevant to the pathophysiology of LQTS and the structure and function of I<sub>Ks</sub> channels are considered.

## METHODS

### Molecular Biology

Human *minK* and *KvLQT1* genes were generous gifts from R. Swanson (Merck, West Point, PA) and M. Keating and M. Sanguinetti (University of Utah, Salt Lake City, UT), respectively (Hice et al., 1994; Sanguinetti et al., 1996b). Mutants of *minK* were produced by plaque-forming unit-based mutagenesis (QuikChange™ Site-Directed Mutagenesis Kit; Stratagene Inc., La Jolla, CA), followed by insertion of mutant gene fragments into translationally silent restriction sites. All sequences were confirmed by automated DNA sequencing. Genes were subcloned into pBF2 (Glowatzki et al., 1995), a gift of Bernd Fakler (University of Tübingen, Tübingen, Germany), and cRNAs transcribed using T3 RNA polymerase and the mMessage mMachine™ kit (Ambion Inc., Austin, TX). Transcripts were quantified by spectroscopy and compared with control samples separated by agarose gel electrophoresis and stained with ethidium bromide. Transient transfection of Chinese Hamster Ovary (CHO) cells was achieved by standard DEAE-Dextran/chloroquine/DMSO methodology using either pAlterMax (Promega Corp., Madison, WI) or pcDNA3 (Invitrogen Corp., San Diego, CA) plasmids carrying the genes for *minK*, *KvLQT1*, or green fluorescent protein.

### Electrophysiology

*Xenopus laevis* oocytes were isolated and injected with 46 nl containing 5 ng *KvLQT1* with or without 1 ng *minK* cRNA. Mixtures

of cRNAs were prepared immediately before injection with a calibrated pipette. Patch currents were recorded 2–3 d after injection using an Axopatch 200A amplifier (Axon Instruments, Foster City, CA), a Quadra 800 computer and ACQUIRE software (Instrutech, Great Neck, NY) and stored unfiltered on VHS tape. The data were filtered through a four-pole Bessel filter for analysis with TAC (Instrutech Corp.) and IGOR (WaveMetrics Inc., Lake Oswego, OR) software packages. Data are displayed without leak subtraction. Unless otherwise stated, the bath solution contained (mM) 100 KCl, 2 EGTA, and 10 HEPES, pH 7.5 with KOH (100 KCl solution). All experiments were performed at 22°C. Data are presented as mean ± SEM with the number of patches indicated in parentheses. Two-electrode voltage clamp was performed with an Oocyte Clamp™ (Warner Instruments, Hamden, CT), an IBM pentium-based personal computer, and pCLAMP software (Axon Instruments). As reported previously, recorded currents show no evidence for contamination of human I<sub>Ks</sub> channels by complexes formed between minK and the KvLQT1 subunit endogenous to oocytes; the two channel types can be differentiated pharmacologically and no channels containing the endogenous subunit are expressed at times >36 h after cRNA injection (Tai and Goldstein, 1998).

### Noise Variance Analysis

A variation of the method of stationary variance analysis (Sigworth and Zhou, 1992) was employed assuming linear dependence of single-channel current on membrane voltage; thus,

$$i_{s.c.} = \gamma(V - V_{rev}), \quad (1)$$

where  $i_{s.c.}$  is single-channel current,  $\gamma$  unitary conductance,  $V$  membrane voltage, and  $V_{rev}$  reversal potential. Unless otherwise stated, the data were sampled at 80 kHz and filtered at 25 kHz at voltages of 10–80 mV in 10-mV steps, and unitary conductances determined by fitting to:

$$\frac{\sigma^2}{I(V - V_{rev})} = -\frac{1}{n} \left( \frac{I}{V - V_{rev}} \right) + \gamma, \quad (2)$$

where  $\sigma^2$  is variance,  $I$  is mean macroscopic current obtained at different voltages, and  $n$  is number of channels in the patch. Mean macroscopic currents ( $I_a$ ) and variances at different voltages were determined from all point amplitude histograms constructed from 400 ms of test data fit to the gaussian function:

$$\exp\left(-\frac{(I - I_a)^2}{2\sigma^2}\right). \quad (3)$$

Progressive reductions (from 400 to 80 ms) in the amount of data subjected to analysis altered measured variance by no more than 5%, indicating that changes in mean current over the sample period were well tolerated. This method differs from that employed by a companion paper by Yang and Sigworth (1998) in that we altered channel open probability ( $P_o$ ) by varying voltage, whereas they assessed changes in  $P_o$  at a single voltage over time. When the same data sets were evaluated by the two methods, the difference unitary current estimates was <15% ( $n = 4$  patches).

I<sub>Ks</sub> currents are characterized by slow development and failure to reach saturation. Thus, all studies were performed using test depolarizations of many seconds duration from a holding voltage of –60 mV to potentials from 10–80 mV. Currents elicited in the first 120 ms of each test pulse showed no time delay and were assumed to be non-channel dependent; these leak currents and their variances were subtracted. Conductance determinations were based on current and variance data collected near the end of the test depolarizations at times >5 s. This protocol was based on assessments of wild-type I<sub>Ks</sub> and KvLQT1 channel conductances at different times during test pulses; in each case, values

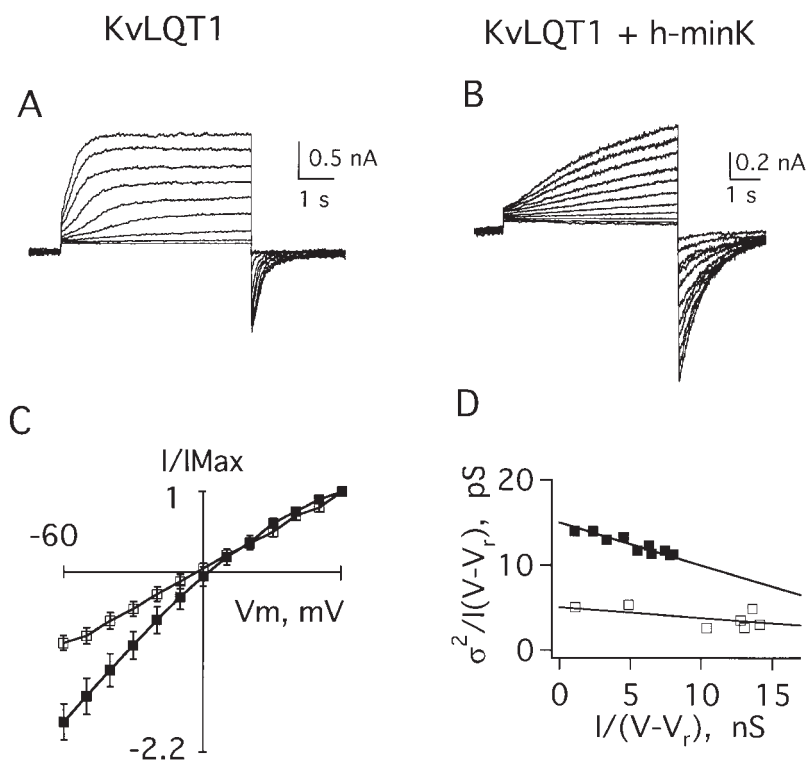


FIGURE 1. Currents recorded in excised inside-out patches containing KvLQT1 or  $I_{Ks}$  channels in symmetrical 100-mM KCl solution. Patches were clamped to  $-60$  mV, and then depolarized for 6 s. (A) KvLQT1 channels depolarized to test potentials of  $0$ – $80$  mV in  $10$ -mV steps. (B)  $I_{Ks}$  channels depolarized to test potentials of  $-20$  to  $80$  mV in  $10$ -mV steps. (C) Peak current–voltage relationship for KvLQT1 channels ( $\square$ ) and  $I_{Ks}$  channels ( $\blacksquare$ ), mean  $\pm$  SEM for three separate patches; see Table I. (D) Variance–current relationship of data in A ( $\square$ , KvLQT1 channels) and B ( $\blacksquare$ ,  $I_{Ks}$  channels); the conductances calculated in these patches were  $4.1$  pS for A, and  $15$  pS for B.

were stable when determined at times longer than 3 s, presumably because large numbers of channels were active at later times and channel currents significantly greater in magnitude than non-channel noise (data not shown).

## RESULTS

### Unitary Conductance of Wild Type KvLQT1 and $I_{Ks}$ Channels

Cloning the gene for *KvLQT1* (Wang et al., 1996b) and

its subsequent overexpression (Sanguinetti et al., 1996b) made possible studies of KvLQT1 and  $I_{Ks}$  channels in excised membrane patches. Fig. 1 A shows a family of macroscopic KvLQT1 currents recorded in a giant inside-out patch excised from an oocyte injected 2 d earlier with *KvLQT1* cRNA. In response to 6-s test pulses from  $-60$  mV to a variety of depolarized potentials, KvLQT1 channels showed fast activation of outward currents and fast deactivation of inward currents (Table I). Under the same conditions,  $I_{Ks}$  channels formed by coassembly of wild-type human minK and KvLQT1

TABLE I  
Conductance, Activation and Deactivation Properties of Homomeric KvLQT1 Channels and Wild-Type and Mutant  $I_{Ks}$  Channels

Channel (No. of patches)	$\gamma$ , pS	Activation $\tau$	$V_{1/2}$ , mV	$Z_0$	I +60 mV I –60 mV	Deactivation $\tau_1$
		$s$	$mV$			$s^{-1}$
KvLQT1 (7)	$4.0 \pm 1.4$	$0.3 \pm 0.1$	$-6 \pm 2$	$2.0 \pm 0.1$	$1.1 \pm 0.2$	$0.4 \pm 0.1$
Wild-type $I_{Ks}$ (15)	$15.6 \pm 4.3$	$5.4 \pm 1.4$	$20 \pm 3$	$1.0 \pm 0.1$	$2.2 \pm 0.3$	$1.2 \pm 0.1$
G55C $I_{Ks}$ (3)	$11.7 \pm 1.9$	$5.6 \pm 0.8$	$19 \pm 1$	$1.1 \pm 0.2$	$2.1 \pm 0.1$	$1.2 \pm 0.1$
D76N + WT $I_{Ks}$ (5)	$8.1 \pm 2.5$	$3.8 \pm 1.3$	$28 \pm 2$	$1.0 \pm 0.1$	$2.5 \pm 0.3$	$0.5 \pm 0.1$
D76N $I_{Ks}$ (8)	$4.8 \pm 1.4$	$2.8 \pm 0.4$	$37 \pm 6$	$1.3 \pm 0.2$	$3.2 \pm 0.5$	$0.3 \pm 0.1$
S74L + WT $I_{Ks}$ (5)	$13.6 \pm 1.5$	$6.6 \pm 1.8$	$34 \pm 4$	$1.1 \pm 0.2$	$2.1 \pm 0.3$	$1.0 \pm 0.2$
S74L $I_{Ks}$ (7)	$8.9 \pm 1.5$	$7.8 \pm 1.8$	$43 \pm 2$	$1.6 \pm 0.1$	$2.1 \pm 0.3$	$0.8 \pm 0.1$
D76N + S74L $I_{Ks}$ (5)	$6.6 \pm 1.2$	$4.0 \pm 0.3$	$39 \pm 3$	$1.3 \pm 0.2$	$2.8 \pm 0.4$	$0.4 \pm 0.1$

Unitary conductance was determined by sampling at 80 kHz and filtering at 25 kHz at test voltages of  $10$ – $80$  mV in  $10$ -mV steps (METHODS). Activation kinetics were estimated from currents measured in macropatches during a 6-s depolarization to  $60$  mV from a holding voltage of  $-60$  mV in symmetrical 100-mM KCl solution; currents were fit by a single exponential function:  $I_0 + I_1 e^{-(t/\tau)}$ . Half maximal activation potentials ( $V_{1/2}$ ) and equivalent valences ( $z_0$ ) were determined by comparing maximal currents at  $60$  and  $-60$  mV in symmetrical 100-mM KCl solution. Deactivation traces were fit with the function:  $I_0 + I_1 e^{-(t/\tau_1)}$ . The values for KvLQT1 and  $I_{Ks}$  correspond to unitary currents at  $50$  mV and  $25$  kHz of  $0.20$  and  $0.78$  pA, respectively.

subunits exhibited slower activation rates, slower deactivation rates (Fig. 1 *B* and Table I) and increased inward rectification (Fig. 1 *C*).

To assess the conductive properties of KvLQT1 and  $I_{Ks}$  channels, a variation of stationary variance analysis (Sigworth and Zhou, 1992) was performed (see METHODS). Unitary conductances ( $\gamma$ ) were determined by fitting collected data to Eqs. 1–3 (Fig. 1 *D*). The average value for KvLQT1 channels was  $4.0 \pm 1.4$  pS (mean  $\pm$  SEM for seven patches), while that for  $I_{Ks}$  channels was  $15.6 \pm 4.3$  pS (mean  $\pm$  SEM for 15 patches, Table I); these correspond to unitary channel currents of 0.20 and 0.78 pA, respectively, at 50 mV. Thus, homomeric KvLQT1 channels passed a unitary current roughly fourfold smaller than  $I_{Ks}$  channels containing wild-type human minK and KvLQT1 subunits.

These estimates suggested it might be possible to observe  $I_{Ks}$  channels directly in inside-out patches. Despite many similarities in single-channel activity and macro-

scopic currents, it was extremely difficult to discern discrete gating transitions of human  $I_{Ks}$  channels. Thus, single channels were inactive at  $-80$  mV, activated slowly at  $40$  mV, and, upon repolarization to  $-80$  mV, were active briefly before deactivation (Fig. 2 *A*). While expansion of the time scale made it possible to appreciate channel activity in comparison to baseline, the “flickery” nature of the channel precluded observation of transitions between closed and open states (Fig. 2 *B*).

Our inability to discern single-channel transitions made it imperative to confirm the activity under scrutiny truly resulted from  $I_{Ks}$  channel function. Support for this identification came first from similarity of microscopic and macroscopic activation kinetics, as judged from comparison of patches with only a few channels (Fig. 3 *A*) assembled in a cumulative fashion (Fig. 3 *B*) and giant patches with many channels (Fig. 3 *C*). A second line of evidence was the observation that single channels in patches passed  $K^+$  but not  $Na^+$  ions, as ex-

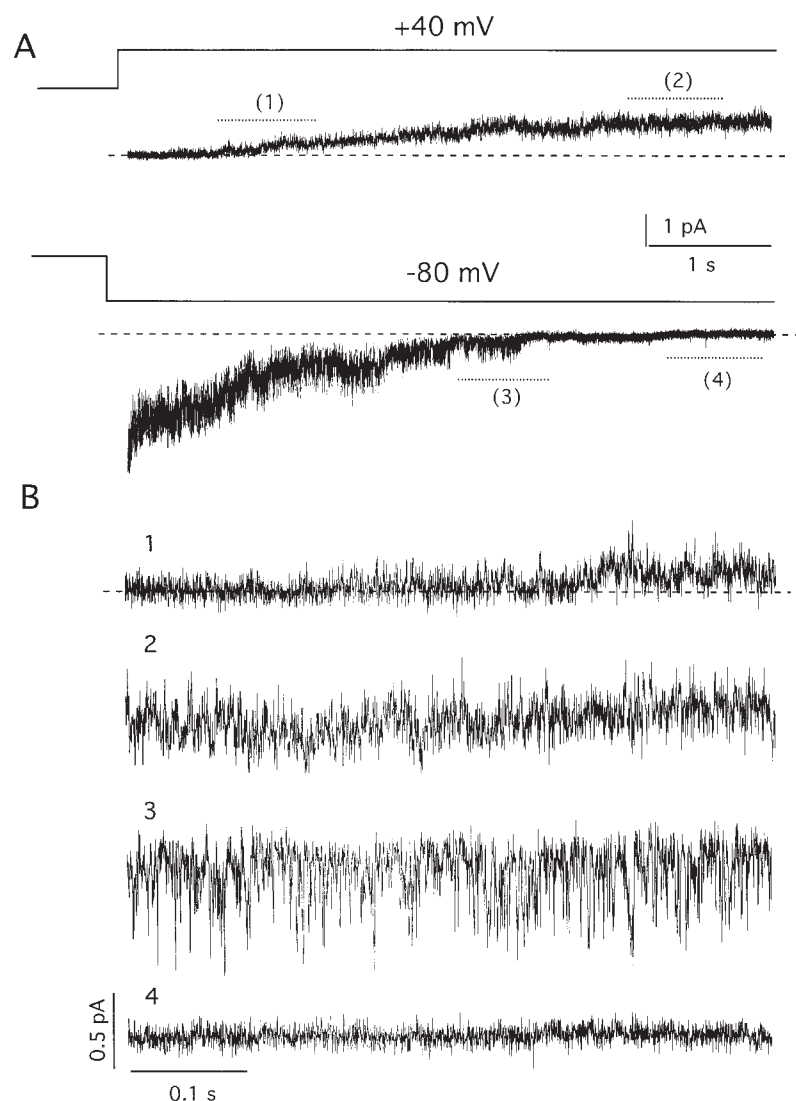


FIGURE 2. Single-channel activity recorded from an inside-out patch containing a few wild-type  $I_{Ks}$  channels in symmetrical 100-mM KCl solution. (A) Current activation at  $40$  mV from a holding voltage of  $-80$  mV. (B) Current deactivation on return to  $-80$  mV. Expanded traces 1–4 are from the indicated portions of A and B. Data were sampled at  $4$  kHz and filtered at  $1$  kHz.

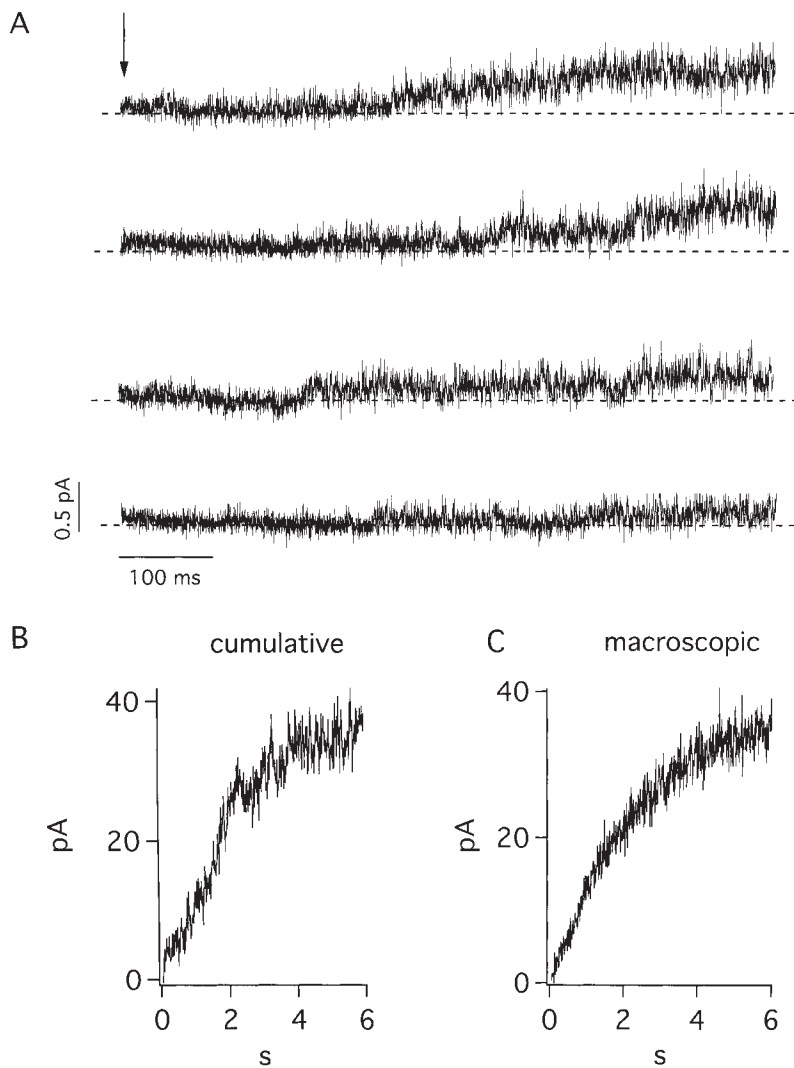


FIGURE 3. Activation of wild-type  $I_{Ks}$  channels in inside-out patches in symmetrical 100-mM KCl solution. (A) Four traces from a patch showing channels opening after depolarization to 40 mV (arrow) from a holding voltage of  $-80$  mV; 600 ms of the 6-s pulse is shown; data sampled at 4 kHz and filtered at 1 kHz. (B) Cumulative current of 30 sweeps of the patch shown in A. (C) Single trace of another patch with many channels by the protocol in B.

pected of  $I_{Ks}$  channels (data not shown). A third experimental support came from studies of a site-directed minK mutant that forms  $I_{Ks}$  channels sensitive to extracellular  $Cd^{2+}$  (Tai and Goldstein, 1998). Previous whole cell studies showed that wild-type  $I_{Ks}$  channels were insensitive to  $Cd^{2+}$ , while channels formed with G55C human minK (altering glycine 55 to cysteine) were blocked by the metal through a pore-occlusion mechanism (Tai and Goldstein, 1998). Here, single  $I_{Ks}$  channels formed with G55C minK were studied in excised patches. The G55C  $I_{Ks}$  channels appear essentially unaltered from wild type in their gating and unitary conductance (Fig. 4, Table I). However, while  $I_{Ks}$  channels carrying wild-type minK were  $Cd^{2+}$  insensitive (Fig. 4 A), single channels containing G55C minK were reversibly inhibited by 1 mM  $Cd^{2+}$  (Fig. 4, B–D).  $I_{Ks}$  channels containing G55C minK, but not wild-type minK, were also sensitive to blockade by external  $Zn^{2+}$  (data not shown). The similarities of microscopic and macroscopic currents in their gating kinetics, ion selectivity,

current rectification, and pharmacology (Figs. 1–4) argued strongly that the rapidly flickering channels under study in excised patches were  $I_{Ks}$  channels.

#### *Gating and Current Rectification of Wild-Type KvLQT1 and $I_{Ks}$ Channels*

Whole-cell studies previously showed that KvLQT1 currents activated rapidly, reached saturation, and deactivated rapidly, whereas  $I_{Ks}$  currents activated slowly, did not saturate, and deactivated slowly (Wang et al., 1996a; Splawski et al., 1997; Tai et al., 1997; Tzounopoulos et al., 1998). Gating behavior of single channels in excised patches reflected these whole-cell findings. Thus, homomeric KvLQT1 channels activated  $\sim 15$ - and deactivated  $\sim 4$ -fold faster than  $I_{Ks}$  channels (Table I). These differences were apparent to the eye (Fig. 1, A and B) and were quantified by comparison of time constants determined from exponential fits to the data (Fig. 5, A and B, Table I). In agreement with earlier re-

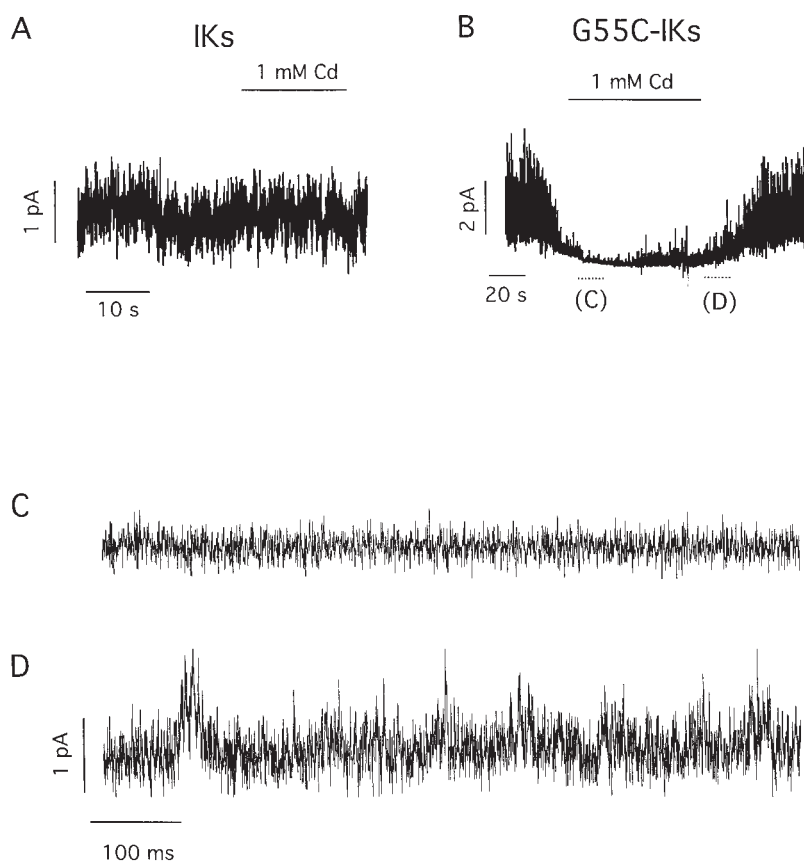


FIGURE 4. Single-channel activity of  $I_{Ks}$  channels formed with wild-type or G55C minK in the presence and absence of external  $Cd^{2+}$ . Currents were recorded in outside-out patches containing a few channels held at 60 mV in symmetrical 100-mM KCl solution. (A)  $I_{Ks}$  channels formed with wild-type minK are insensitive to 1 mM  $Cd^{2+}$  (exposure indicated by bar). (B)  $I_{Ks}$  channels formed with G55C minK are blocked by 1 mM  $Cd^{2+}$  (exposure indicated by bar). (C and D) Expanded traces from the indicated portions of B. Sampled at 4 kHz, filtered at 30 Hz (A and B), or 1 kHz (C and D).

ports of whole-cell current activation (Sanguinetti et al., 1996b),  $I_{Ks}$  channels in excised patches were less sensitive to voltage than KvLQT1 channels, showing a half-maximal activation potential 25 mV more positive and a normalized open probability–voltage relationship that was more shallow (Fig. 5 A, Table I). Normalized tail current plots make apparent that KvLQT1 channels deactivated more rapidly than wild-type  $I_{Ks}$  channels (Fig. 5 B, Table I).

#### Unitary Conductance of $I_{Ks}$ Channels Containing MinK Mutants that Cause LQTS

Recently, mutant genes encoding D76N minK and S74L minK were identified in patients with LQTS (Splawski et al., 1997; Duggal et al., 1998). In some patients, LQTS was inherited in an autosomal dominant fashion and affected individuals possessed one normal and mutant allele. Thus, we first studied the influence of minK mutants on  $I_{Ks}$  function using oocytes injected with cRNAs for KvLQT1 subunits and a 1:1 mixture of wild-type and mutant minK subunits. Thereafter, to study a single population of channels, oocytes were injected with cRNAs for KvLQT1 subunits and a minK mutant in the absence of wild-type minK. The current in Fig. 6 A was recorded in an excised patch from a cell

injected with cRNAs for KvLQT1, D76N minK, and wild-type minK (to approximate the subunit composition of myocytes of individuals with D76N minK-associated LQTS). In this case, the conductance was a weighted average from a mixture of  $I_{Ks}$  channels (some with only wild-type minK, some only mutant minK, others with both). The apparent conductance was  $8.1 \pm 2.5$  pS (Table I, Fig. 6 D). Clearly, this experiment did not offer insight into the properties of any individual channel type in the patch.

Fig. 6 B shows the current from oocytes expressing  $I_{Ks}$  channels formed with KvLQT1 and D76N minK subunits. Current–variance analyses estimated the unitary conductance of these channels to be  $4.8 \pm 1.4$  pS (Table I, Fig. 6 C). D76N  $I_{Ks}$  channels also showed greater inward rectification than wild-type channels (Table I, Fig. 6 D).

Fig. 6 E shows the effect of progressively increasing the relative amount of D76N minK cRNA with respect to wild type. Increasing the proportion of D76N minK subunits caused a decreased average unitary conductance. This indicated that D76N  $I_{Ks}$  channels and mixed D76N/wild-type  $I_{Ks}$  channels were both functional and that more than one minK subunit was present in each channel complex. A quantitative consideration of this data in relation to subunit stoichiometry is below (DISCUSSION).



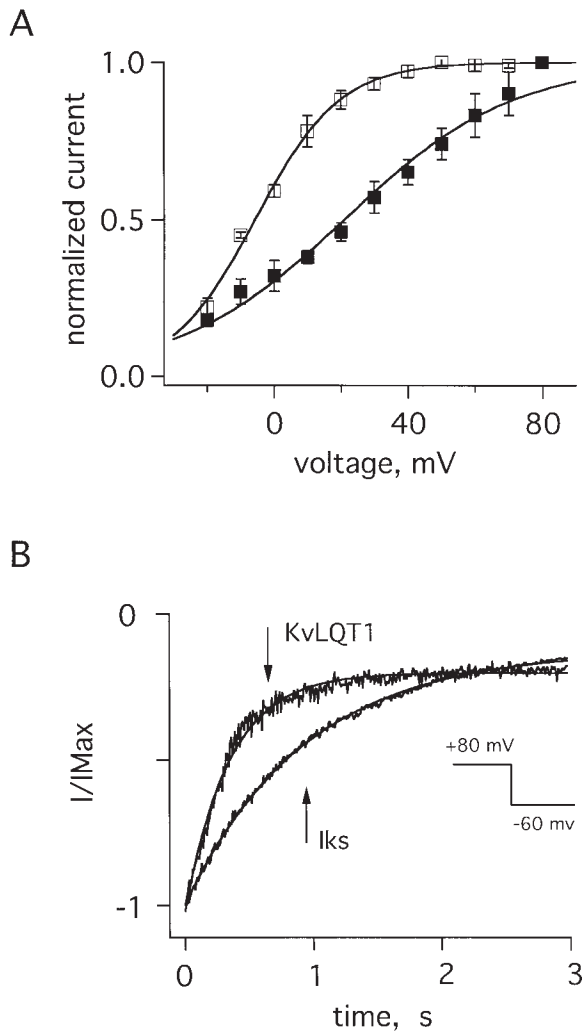


FIGURE 5. Gating attributes of KvLQT1 and  $I_{Ks}$  channels in excised patches. (A) Normalized open probabilities ( $I/IMax$ ) for KvLQT1 channels ( $\square$ ) and  $I_{Ks}$  channels ( $\blacksquare$ ). Peak tail current at  $-60$  mV was measured after a 6-s prepulse to voltages of  $-20$  to  $80$  mV. The curves are normalized to  $80$ -mV prepulse value. Theoretical lines are constructed with the Boltzmann function:  $1/[1 + \exp\{ez(V_{1/2} - V)/kT\}]$ , where  $z$  is the equivalent valence,  $e$  the elementary charge,  $V_{1/2}$  the voltage at which the curve is half maximal (see Table I),  $k$  the Boltzmann constant, and  $T$  the absolute temperature; for KvLQT1 channels,  $z = 2.0 \pm 0.1$ ; for  $I_{Ks}$  channels,  $z = 1.0 \pm 0.1$ . (B) Normalized tail currents in a patch at  $-60$  mV. Currents were elicited by a 6-s pulse to  $80$ -mV voltage (inset). Theoretical lines are single exponential fits to the deactivation time course; results from many patches are in Table I.

A second group of patients with LQTS carries one mutant gene encoding S74L minK subunits and one wild-type gene. Currents resulting from coexpression of *KvLQT1* cRNA and a 1:1 mixture of S74L and wild-type *minK* cRNAs gave an average conductance of  $13.6 \pm 1.5$  pS (Table I, Fig. 7, A and D). As before, this was an average conductance for a number of channel types. Analyses carried out on oocytes injected

with just *KvLQT1* and S74L *minK* cRNAs showed S74L  $I_{Ks}$  channels to have a unitary conductance of  $8.9 \pm 1.5$  pS (Table I, Fig. 7, B and D). Unlike D76N  $I_{Ks}$  channels, S74L channels showed current rectification similar to wild type (Table I, Fig. 7 C).

A third group of patients (with Jervell and Lange-Nielsen Syndrome or Romano-Ward Syndrome) manifest both LQTS and hearing defects (Schulze-Bahr et al., 1997; Duggal et al., 1998); these individuals carry two mutant alleles of *minK*. When oocytes were coinjected with cRNAs for *KvLQT1* and a 1:1 mixture of D76N and S74L *minK* cRNAs (as seen in some of these individuals), the resulting channels had an average unitary conductance of  $6.6 \pm 1.2$  pS (Table I, Fig. 8, A and C). These channel mixtures showed average conductance and rectification properties intermediate in phenotype to pure D76N and S74L  $I_{Ks}$  channels (Table I, Fig. 8, B and C).

#### Gating of $I_{Ks}$ Channels Containing *minK* Mutants

While activation of wild-type  $I_{Ks}$  channels proceeded about half as fast as D76N channels and twice as fast as S74L channels, all  $I_{Ks}$  channels activated more slowly than homomeric KvLQT1 channels (Table I). Compared with wild-type  $I_{Ks}$  channels, the half-maximal activation potential for D76N and S74L channels was shifted to more depolarized voltages (Fig. 9 A, Table I). Deactivation of D76N  $I_{Ks}$  channels was significantly faster and S74L channels moderately faster than wild-type channels (Fig. 9 B, Table I), in good agreement with an earlier report (Splawski et al., 1997). Patches from cells expressing both D76N and S74L *minK* showed activation kinetics that were intermediate to those of pure D76N or S74L channels (Table I), but speeded deactivation kinetics similar to D76N channels (Fig. 9 B, Table I). These results were consistent with the idea that KvLQT1 could assemble with either D76N or S74L minK subunits to form functional mutant  $I_{Ks}$  channels characterized by small unitary currents, altered gating kinetics and marked inward rectification (Table I).

#### Selectivity of $I_{Ks}$ Channels Containing MinK Mutants that Cause LQTS

As coassembly altered unitary conductances, we sought evidence for changes in ion selectivity, another pore-determined channel attribute. The relative permeabilities of monovalent cations similar to  $K^+$  ion were assessed using biionic reversal potential measurements in whole-cell configuration. Wild-type  $I_{Ks}$  channels showed the same permeability series as KvLQT1 channels ( $K^+ > Rb^+ > NH_4^+ > Cs^+ \gg Li^+, Na^+$ ), but a slightly greater selectivity against  $NH_4^+$  and  $Cs^+$  (Table II), as found by others (Wollnik et al., 1997). While mutation



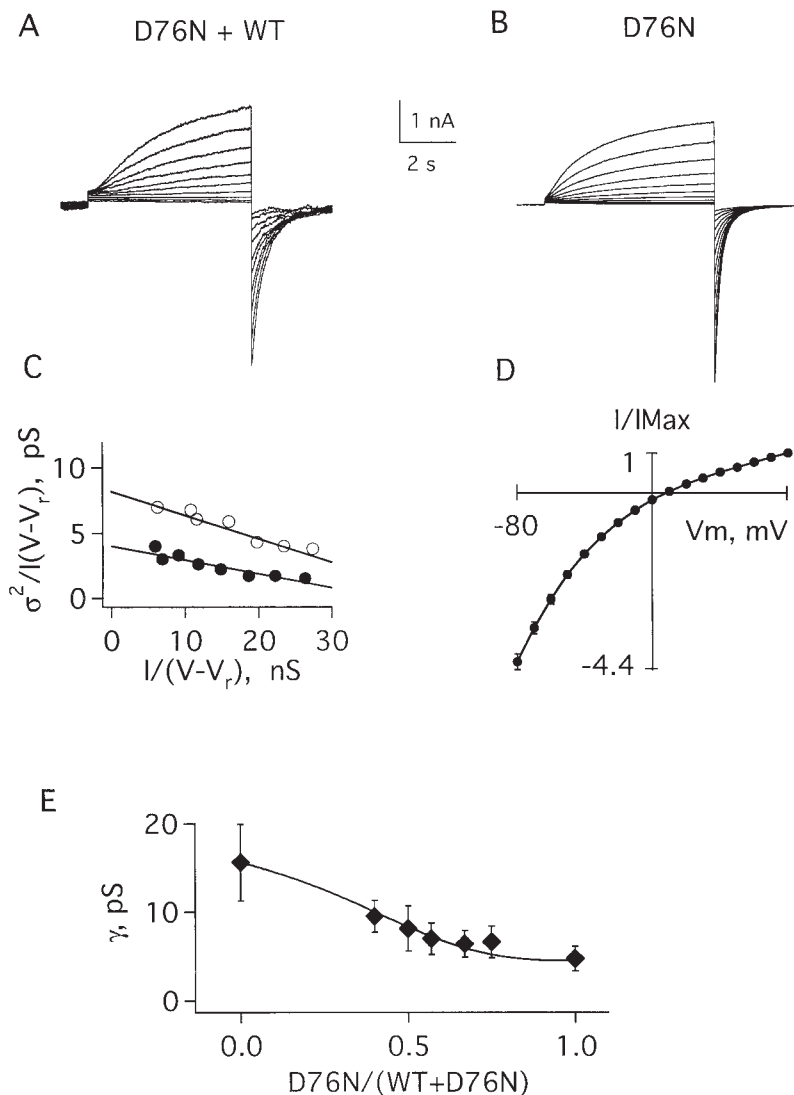


FIGURE 6. Current-variance relationships of  $I_{Ks}$  channels formed with wild-type and D76N minK subunits. (A) Family of currents recorded in a patch excised from an oocyte coinjected with KvLQT1 cRNA and a 1:1 mixture of wild-type and D76N minK cRNAs. The patch was clamped at  $-60$  mV and depolarized from  $-20$  to  $70$  mV in  $10$ -mV steps. (B) Family of currents recorded from oocytes coinjected only with KvLQT1 and D76N minK cRNAs. The protocol was similar to A, except that test pulses were up to  $80$  mV. (C) Current-variance relationships computed from the patches in A ( $\circ$ ) and B ( $\bullet$ ); the conductances calculated in these patches were  $8.2$  and  $4.0$  pS, respectively. (D) Current-voltage relationship of peak tail currents measured for D76N  $I_{Ks}$  channels, mean  $\pm$  SEM for four patches. (E) Dependence of unitary conductance on the fraction of injected wild-type and D76N cRNAs. The theoretical line was constructed according to Eqs. 4-6 with a best fit yielding a maximal value of  $n = 2.8$  minK subunits per channel (see DISCUSSION).

of human minK position G56 increased permeation of  $I_{Ks}$  channels by  $\text{Na}^+$  ion fivefold (Tai and Goldstein, 1998), and mutation of rat minK position F55 increased permeation by  $\text{NH}_4^+$  and  $\text{Cs}^+$  threefold (Goldstein and Miller, 1991), neither D76N nor S74L channels showed changes in ion discrimination (Table II). Thus, these LQTS-associated mutations at positions S74 and D76 altered single-channel conductance (and gating) without effecting function of the ion selectivity filter.

#### Unitary Conductance of Wild-Type KvLQT1 and $I_{Ks}$ Channels in CHO Cells

To ascertain whether unitary current magnitudes varied when channels were in mammalian cells rather than oocytes, we reassessed the current variance of KvLQT1 and  $I_{Ks}$  channels expressed in CHO cells (Fig. 10). Unitary conductances in CHO cells were  $2.3 \pm 0.6$  pS ( $n = 4$  cells) and  $7.9 \pm 1.3$  pS ( $n = 3$  cells) for

KvLQT1 and  $I_{Ks}$  channels, respectively; this corresponds to unitary currents of  $0.20$  and  $0.79$  pA with a  $50$ -mV driving force, the same as we found for the channels in oocytes at  $25$  kHz (Table I, Fig. 1).

#### DISCUSSION

To gain insight into the mechanisms underlying their function, we have analyzed the currents recorded from channels formed only with KvLQT1 subunits and those coassembled from human minK and KvLQT1 subunits to form  $I_{Ks}$  channels. Noise-variance analyses showed the mixed channel complex to have a unitary conductance fourfold greater than that of homomeric KvLQT1 channels (Table I). As expected,  $I_{Ks}$  channels were found to activate and deactivate more slowly, to be less sensitive to voltage, and to select slightly more effectively against  $\text{Cs}^+$  and  $\text{NH}_4^+$  ions than KvLQT1 channels (Tables I and II). When mutant  $I_{Ks}$  channels were formed with two minK subunits associated with LQTS

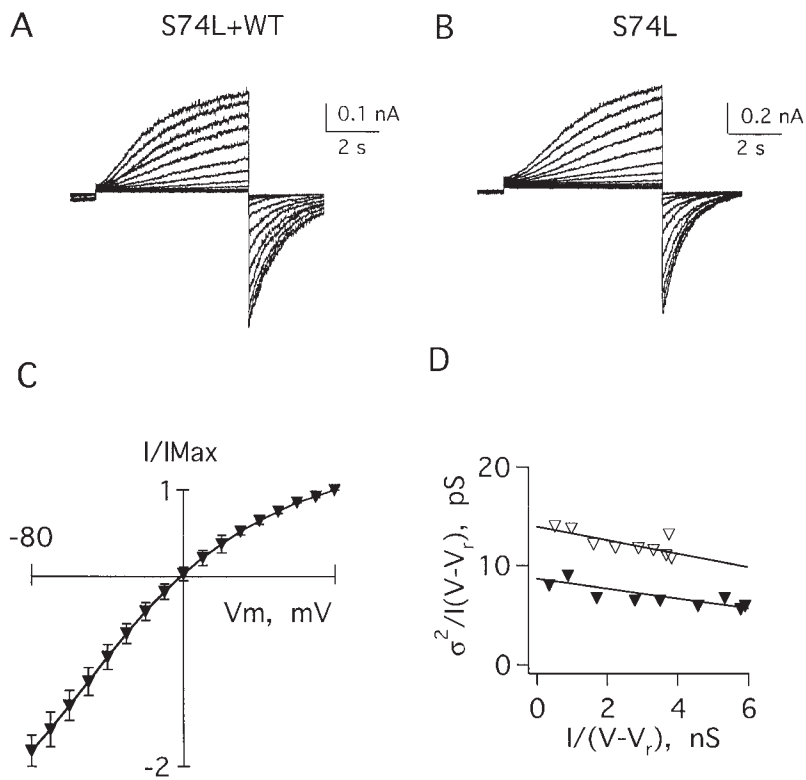


FIGURE 7. Current-voltage relationships of  $I_{Ks}$  channels formed with wild-type and S74L minK subunits. (A) Family of currents recorded in a patch excised from an oocyte coinjected with KvLQT1 cRNA and a 1:1 mixture of wild-type and S74L minK cRNAs. The patch was clamped at  $-60$  mV and depolarized from  $-20$  to  $100$  mV in steps of  $10$  mV. (B) Family of currents recorded from oocytes coinjected only with KvLQT1 and S74L minK cRNAs. The protocol was as in A with steps from  $-20$  to  $90$  mV. (C) Current-voltage relationship of peak tail currents measured for S74L  $I_{Ks}$  channels, mean  $\pm$  SEM for three patches. (D) Current-variance relationships computed from the patches in A ( $\nabla$ ) and B ( $\blacktriangledown$ ); the conductances calculated in these patches were  $14$  and  $8.7$  pS, respectively.

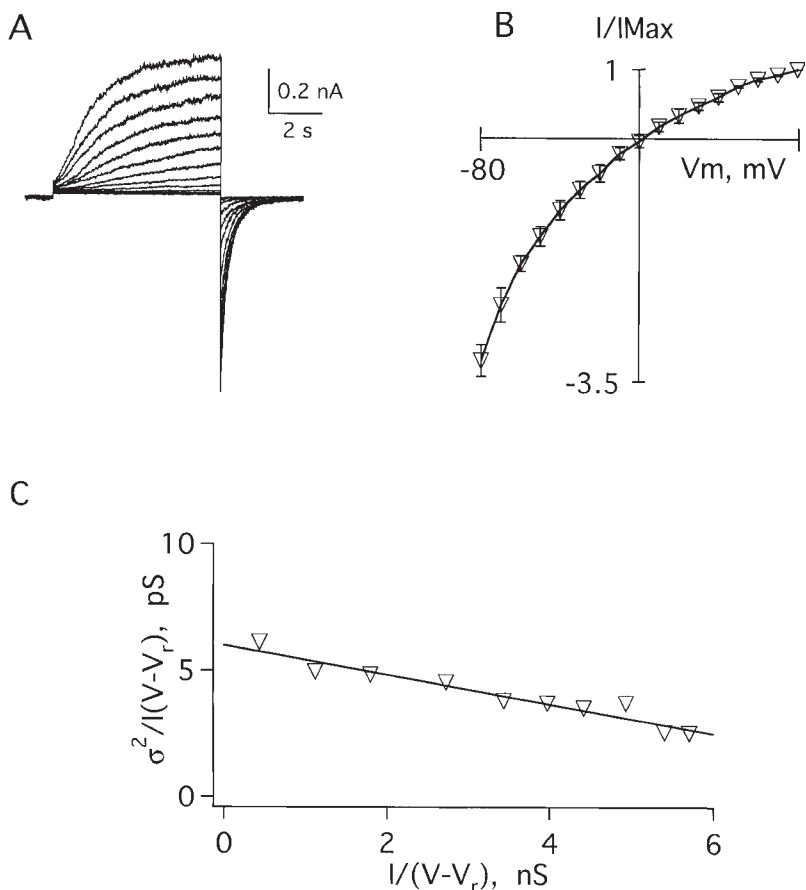


FIGURE 8. Current-voltage relationships of  $I_{Ks}$  channels formed with S74L and D76N minK subunits. (A) Family of currents recorded from a patch excised from an oocyte coinjected with KvLQT1 cRNA and a 1:1 mixture of D76N and S74L minK cRNAs. The patch was clamped at  $-60$  mV and depolarized from  $-20$  to  $100$  mV in  $10$ -mV steps. (B) Current-voltage relationship of peak tail currents measured for channels, mean  $\pm$  SEM for three separate patches. (C) Current-variance relationship computed from the patch in A; the conductance calculated in this patch was  $6.0$  pS.

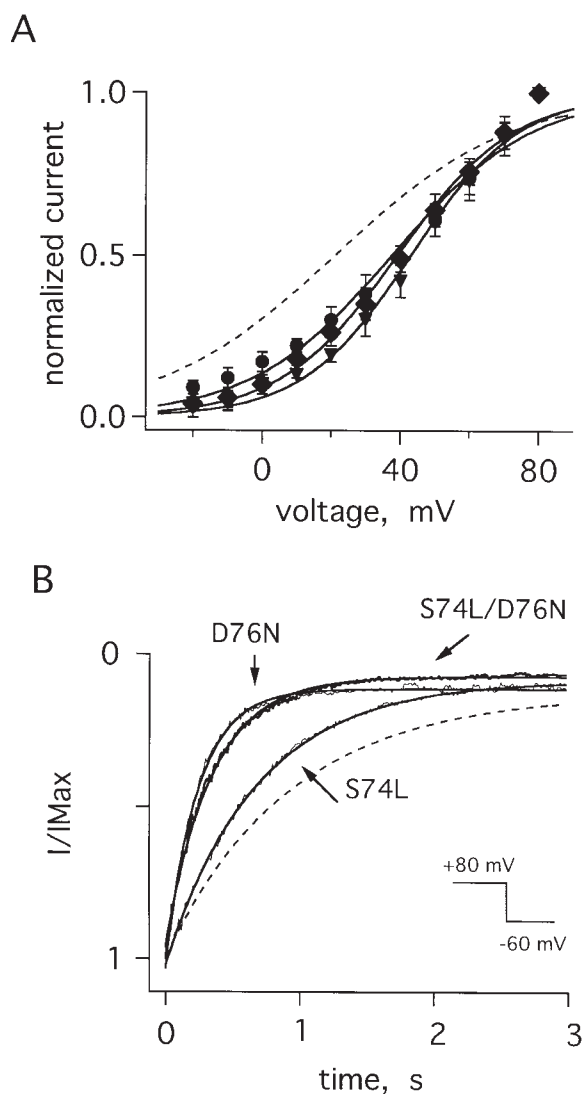


FIGURE 9. Gating attributes of mutant  $I_{Ks}$  channels. (A) Normalized open probabilities ( $I/I_{max}$ ) for cells with D76N  $I_{Ks}$  channels ( $\bullet$ ,  $z = 1.3 \pm 0.2$ ), S74L  $I_{Ks}$  channels ( $\blacktriangledown$ ,  $z = 1.6 \pm 0.1$ ), and S74L-D76N  $I_{Ks}$  channels ( $\blacklozenge$ ,  $z = 1.3 \pm 0.2$ ); protocols, theoretical fits, and equivalent valences ( $z$ ) as in Fig. 5; the dotted line is the curve for wild-type  $I_{Ks}$  channels from Fig. 5 A. (B) Normalized tail currents at  $-60$  mV for D76N, S74L, and D76N-S74L  $I_{Ks}$  channels; the dotted line is the curve for wild-type  $I_{Ks}$  channels from Fig. 5 B. Currents were elicited after a 6-s test pulse to 80 mV. Theoretical lines were constructed as described in the legend to Table I.

and compared with wild-type  $I_{Ks}$  channels, they showed lower unitary conductances, a requirement for larger depolarizations to activate, and more rapid deactivation but no significant change in the relative permeability of monovalent cations (Tables I and II).

Our results generally agree with those of Yang and Sigworth (1998), who found coassembly of minK and KvLQT1 to increase single-channel conductance approximately fivefold. While our conductance values are higher than theirs ( $\sim 16$  vs. 5 pS for human  $I_{Ks}$  channels

in oocytes at 25 kHz), this can largely be understood by their use of 7 mM external KCl where we employ symmetrical 100 mM KCl solutions. Indeed, unitary currents should be similar with strong depolarization despite external KCl differences and this was found; Yang and Sigworth (1998) estimated a unitary current for human  $I_{Ks}$  channels at 50 mV and 25 kHz of  $0.6 \pm 0.2$  pA where we found  $0.8 \pm 0.2$  pA (Table I). These results stand in stark contrast to a report that KvLQT1 channels in mammalian cells have a unitary conductance 13-fold larger than  $I_{Ks}$  channels (which were attributed a value of just 0.076 pA) (Romey et al., 1997). To ascertain whether this discrepancy was due to expression of the channels in mammalian cells, we performed current-variance analysis using CHO cells. Consistent with our findings in oocytes (Table I), unitary  $I_{Ks}$  currents in CHO cells were  $\sim 0.8$  pA at 25 kHz, fourfold larger than KvLQT1 channels (Fig. 10). There was also reasonable agreement, considering species and methodologic differences, between the conductance of native  $I_{Ks}$  channels studied in guinea pig cardiac myocytes (Walsh et al., 1991) or stria vascularis (Shen and Marcus, 1998) and our estimate for human channels, as they were  $\sim 50\%$  smaller and  $\sim 20\%$  larger, respectively.

A potential source of error in our measurements was contamination by endogenous currents. This was especially important to consider, as human  $I_{Ks}$  channels were flickery, making it difficult to discern single-channel transitions. However, the channels under study were firmly identified based on their presence in oocytes only after co-injection of *minK* and *KvLQT1* cRNAs, similarity of their gating kinetics to macroscopic  $I_{Ks}$  currents, their selectivity for  $K^+$  ions, and their sensitivity to block by transition metals when formed with G55C minK, in keeping with earlier macroscopic studies (Tai and Goldstein, 1998).

Another source of concern, given the volatile nature of the channel (and our inability to compute amplitude histograms), was the validity of current-variance analyses. In particular, could noise analysis differentiate changes in channel gating from changes in unitary conductance? Could KvLQT1 channels have a conductance as large as  $I_{Ks}$  channels, but flicker more rapidly? To address this issue, we studied the dependence of the variance on experimental bandwidth. According to Eq. 2, the variance and unitary conductance depend on filter frequency in the same fashion. Thus, increasing the bandwidth should cause similar changes in the variance and conductance until the bandwidth increases above a level sufficient to record complete open-closed transitions; at this point, the conductance should "level-off" and approach its maximal "true" value. Fig. 11 shows such an experiment in which data was sampled at 80 kHz, noise-variance was measured, and unitary con-

TABLE II  
Biionic Reversal Potentials and Relative Permeabilities of Wild-Type and Mutant  $I_{Ks}$  Channels

Channel	Na <sup>+</sup>	Li <sup>+</sup>	Cs <sup>+</sup>	NH <sub>4</sub> <sup>+</sup>	Rb <sup>+</sup>	K <sup>+</sup>
KvLQT1	-105 ± 9 (61)	-97 ± 7 (46)	-52 ± 6 (8)	-38 ± 5 (4)	-14 ± 5 (2)	-1 ± 1
Wild-type $I_{Ks}$	-97 ± 9 (48)	-92 ± 9 (43)	-67 ± 5 (15)	-51 ± 5 (8)	-17 ± 6 (2)	2 ± 3
D76N $I_{Ks}$	-95 ± 8 (45)	-95 ± 8 (45)	-48 ± 4 (7)	-47 ± 6 (7)	-7 ± 6 (1)	-1 ± 4
S74L $I_{Ks}$	-100 ± 7 (55)	-101 ± 8 (57)	-54 ± 6 (9)	-42 ± 4 (5)	-7 ± 4 (1)	4 ± 4

Reversal potentials were measured with 100 mM of the indicated cation in the external solution; whole cell currents were elicited by a 6-s command pulse to 30 mV from a holding voltage of -80 mV, followed by repolarization to various test potentials and the slopes of tail currents calculated. Permeability ratios (in parenthesis) are calculated according to  $P_K/P_X = \exp(-FV_{rev}/RT)$ , where  $R$ ,  $T$ , and  $F$  have their usual meanings and  $P_K$  and  $P_X$  are the permeability of K<sup>+</sup> and the test ion, respectively; this assumes that K<sup>+</sup> is the only permeant ion inside the oocyte. Values are mean ± SEM for four to nine oocytes.

ductance calculated as a function of bandwidth from 0.25 to 25 kHz. Above 10 kHz, the calculated conductances for KvLQT1 channels and wild-type and mutant  $I_{Ks}$  channels appeared to approach maximal values. Moreover, the conductances appeared to rise in parallel, suggesting that flicker kinetics were the same in the four channel types studied (homomeric KvLQT1, wild-

type  $I_{Ks}$ , D76N  $I_{Ks}$ , and S74L  $I_{Ks}$  channels). This conclusion is also supported by observation that single  $I_{Ks}$  channels (Figs. 2–4) exhibit the same apparent single-channel conductance as was determined by noise analysis at the analogous bandwidth. Thus,  $I_{Ks}$  channel activity at 1 kHz (Figs. 2–4) showed a unitary current of ~0.3 pA, a bandwidth where the current–variance

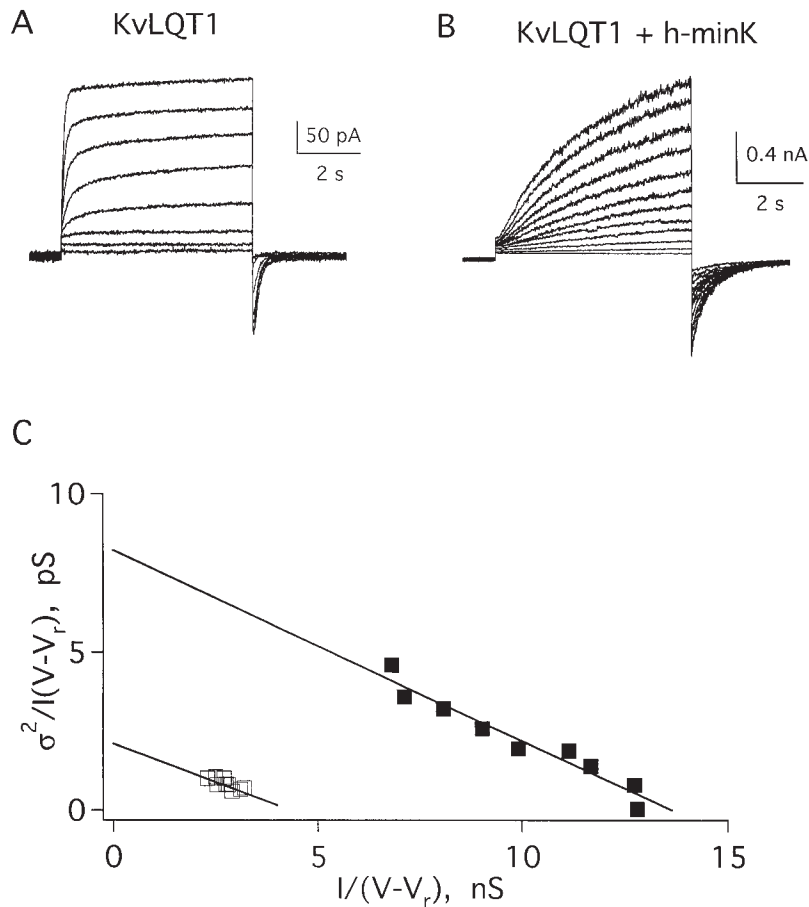


FIGURE 10. Currents recorded in CHO cells expressing KvLQT1 or  $I_{Ks}$  channels by whole-cell configuration. Cells were clamped to -80 mV, and then depolarized for 6 s to test potentials from -60 to 10 mV (KvLQT1) or -60 to 50 mV ( $I_{Ks}$ ) in 10-mV steps. The solutions were (mM): bath: 20 KCl, 100 NaCl, 1 CaCl<sub>2</sub>, 2 MgCl<sub>2</sub>, 10 HEPES, pH 7.5; pipette: 120 KCl, 2 MgCl<sub>2</sub>, 2 EGTA, 10 HEPES, pH 7.5. (A) KvLQT1 channels. (B)  $I_{Ks}$  channels. (C) Variance–current relationships of data in A (□, KvLQT1 channels) and B (■,  $I_{Ks}$  channels). The calculated conductances in these patches were 2.2 and 8.2 pS, respectively.

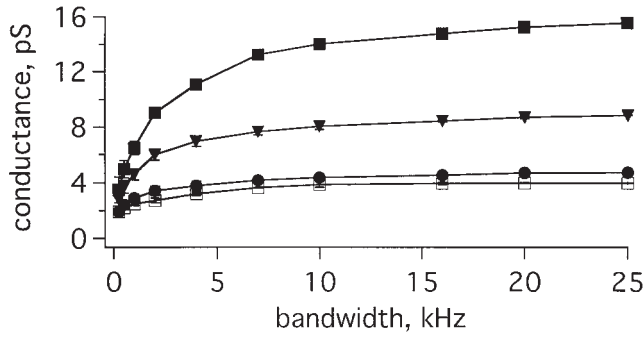


FIGURE 11. Calculated unitary conductances as a function of the experimental bandwidth. Curves shown for KvLQT1 channels ( $\square$ ),  $I_{Ks}$  channels ( $\blacksquare$ ), D76N  $I_{Ks}$  channels ( $\bullet$ ), and S74L  $I_{Ks}$  channels ( $\blacktriangledown$ ). The curves were obtained measuring the variance at 70 mV, using cut-off frequencies from 0.25 to 25 kHz, and then scaled the value of conductance determined at 25 kHz. Data were sampled at 80 kHz and digitally filtered at the indicated frequencies. Each curve represents the average of three patches.

method estimates  $\sim 0.26$  pA. This effect of bandwidth has been seen in other rapidly flickering channels (Sesti et al., 1994).

Mutant  $I_{Ks}$  channels containing D76N and/or S74L minK subunits showed a significant decrease in unitary current when expressed singly or, in an approximation of the clinical situation, in a 1:1 mixture with wild-type minK (Table I). The mutants also shifted the current-voltage relationship for activation to more depolarized potentials and speeded the time course of channel deactivation, as expected from the work of Splawski et al. (1997). Our observation that D76N  $I_{Ks}$  channels were functional, albeit with decreased conductance and lowered open probability, was discrepant with Splawski et al. (1997) and our own earlier experience with an analogous rat mutant (D77N) that suppressed function of channels formed by wild-type rat minK and a KvLQT1-like subunit endogenous to oocytes; this may be attributable to differences in human KvLQT1 and the *Xenopus* protein, as we have seen before (Tai et al., 1997).

As D76N and wild-type minK produced  $I_{Ks}$  channels with different conductances, we asked whether these variations could be used to estimate minK subunit stoichiometry (Fig. 6 E). If we assume no change in open probability with different minK subunit compositions, and that the distribution, half-life, and assembly of  $I_{Ks}$  channels is subunit independent, we can apply a binomial distribution to the analysis (MacKinnon, 1991; Wang and Goldstein, 1995). If we make the further assumption that all channels that are not fully wild type have the low conductance of fully D76N channels, we can estimate an upper limit for the number ( $n$ ) of minK subunits in a complex and express the current and variance as:

$$I = I_{wt} \left[ \frac{(f_{wt}\gamma_{wt} - f_{D76N}\gamma_{D76N})}{\gamma_{wt}} \right] \quad (4)$$

and

$$\sigma^2 = \sigma_{wt}^2 \left[ \frac{(f_{wt}\gamma_{wt}^2 - f_{D76N}\gamma_{D76N}^2)}{\gamma_{wt}^2} \right], \quad (5)$$

where  $f_{wt} = [wt]^n$  is the fraction of injected cRNA that is wild type and  $f_{D76N} = 1 - [wt]^n$  is the cRNA fraction that is mutant. After substituting Eqs. 4 and 5 into Eq. 2, the variance-mean fit yields an apparent single-channel conductance:

$$\gamma = \gamma_{wt} \left[ \frac{f_{wt}\gamma_{wt}^2 + f_{D76N}\gamma_{D76N}^2}{f_{wt}\gamma_{wt} + f_{D76N}\gamma_{D76N}} \right]. \quad (6)$$

A fit to the data in Fig. 6 E gives a value for  $n$  of 2.8. An upper estimate of 3 agrees well with our earlier study suggesting that two rat minK subunits are present in  $I_{Ks}$  channels formed with the KvLQT1-like subunit endogenous to oocytes (Wang and Goldstein, 1995). While our estimates argue against a very large number of minK subunits in each complex (Tzounopoulos et al., 1995), the assumptions underlying the models are unproven. It seems reasonable to conclude that  $I_{Ks}$  channels contain at least two but not more than four minK subunits.

There were three effects of forming  $I_{Ks}$  channels with mutant minK subunits: single-channel conductance was decreased,  $V_{1/2}$  for activation was shifted to more depolarized voltages, and deactivation kinetics were faster. Each of these effects decreased  $K^+$  flux through  $I_{Ks}$  channels, the same mechanism by which mutations in other  $K^+$  channels have been demonstrated to induce LQTS (Sanguinetti et al., 1995, 1996a,b; Keating and Sanguinetti, 1996a,b). The result of decreased  $K^+$  flux is to slow phase 3 repolarization, prolong the cardiac action potential, and increase the QT interval measured on a surface electrocardiogram (Roden et al., 1996).

The data also provide some indirect information about the structure of the  $I_{Ks}$  channel pore. In the past, we found that rat minK residues 55, 56, 57, and 59 (in the midst of single transmembrane segment) were exposed in the ion conduction pathway of  $I_{Ks}$  channels (Tai and Goldstein, 1998); these sites appeared to reside in close proximity to the ion selectivity filter as 55 and 56 were accessible only from the external solution, 57 and 59 were accessible only from the cytosol, and changes at 56 altered  $Na^+$  permeability. Here we find that the mutation of residue 74 or 76 changes single-channel conductance without altering ion selectivity. This suggests these two sites are in the pore but reside at a distance from the selectivity-determining apparatus.

We are grateful to Nicolas Goldstein, Fred Sigworth, and Yousan Yang for their thoughtful comments and enthusiasm.

This work was supported by grants from the National Institutes of Health-National Institute of General Medical Sciences to S.A.N. Goldstein.

Original version received 31 July 1998 and accepted version received 14 October 1998.

## REFERENCES

- Ackerman, M.J. 1998. The long QT syndrome: ion channel diseases of the heart. *Mayo Clin. Proc.* 73:250–269.
- Barhanin, J., F. Lesage, E. Guillemare, M. Fink, M. Lazdunski, and G. Romey. 1996. K(V)LQT1 and Isk (minK) proteins associate to form the I(Ks) cardiac potassium current. *Nature*. 384:78–80.
- Doyle, D.A., J.M. Cabral, R.A. Pfuetzner, A.L. Kuo, J.M. Gulbis, S.L. Cohen, B.T. Chait, and R. Mackinnon. 1998. The structure of the potassium channel—molecular basis of K<sup>+</sup> conduction and selectivity. *Science*. 280:69–77.
- Duggal, P., M.R. Vesely, D. Wattanasirichaigoon, J. Villafane, V. Kaushik, and A.H. Beggs. 1998. Mutation of the gene for Isk associated with both Jervell and Lange-Nielsen and Romano-Ward forms of Long-QT syndrome. *Circulation*. 97:142–146.
- Dumaine, R., Q. Wang, M.T. Keating, H.A. Hartmann, P.J. Schwartz, A.M. Brown, and G.E. Kirsch. 1996. Multiple mechanisms of Na<sup>+</sup> channel-linked long-QT syndrome. *Circ. Res.* 78: 916–924.
- Glowatzki, E., G. Fakler, U. Brandle, U. Rexhausen, H.P. Zenner, J.P. Ruppersberg, and B. Fakler. 1995. Subunit-dependent assembly of inward-rectifier K<sup>+</sup> channels. *Proc. R. Soc. Lond. B Biol. Sci.* 261:251–261.
- Goldstein, S.A., and C. Miller. 1991. Site-specific mutations in a minimal voltage-dependent K<sup>+</sup> channel alter ion selectivity and open-channel block. *Neuron*. 7:403–408.
- Hice, R.E., K. Folander, J.J. Salata, J.S. Smith, M.C. Sanguinetti, and R. Swanson. 1994. Species variants of the Isk protein: differences in kinetics, voltage dependence, and La<sup>3+</sup> block of the currents expressed in *Xenopus* oocytes. *Pflügers Arch.* 426:139–145.
- Keating, M.T., and M.C. Sanguinetti. 1996a. Molecular genetic insights into cardiovascular disease. *Science*. 272:681–685.
- Keating, M.T., and M.C. Sanguinetti. 1996b. Pathophysiology of ion channel mutations. *Curr. Opin. Genet. Dev.* 6:326–333.
- MacKinnon, R. 1991. Determination of the subunit stoichiometry of a voltage-activated potassium channel. *Nature*. 350:232–235.
- Roden, D.M., R. Lazzara, M. Rosen, P.J. Schwartz, J. Towbin, and G.M. Vincent. 1996. Multiple mechanisms in the Long-QT syndrome—current knowledge, gaps, and future directions. *Circulation*. 94:1996–2012.
- Romey, G., B. Attali, C. Chouabe, I. Abitbol, E. Guillemare, J. Barhanin, and M. Lazdunski. 1997. Molecular mechanism and functional significance of the minK control of the KvLQT1 channel activity. *J. Biol. Chem.* 272:16713–16716.
- Sanguinetti, M.C., M.E. Curran, P.S. Spector, and M.T. Keating. 1996a. Spectrum of HERG K<sup>+</sup>-channel dysfunction in an inherited cardiac arrhythmia. *Proc. Natl. Acad. Sci. USA*. 93:2208–2212.
- Sanguinetti, M.C., M.E. Curran, A. Zou, J. Shen, P.S. Spector, D.L. Atkinson, and M.T. Keating. 1996b. Coassembly of K(V)Lqt1 and minK (Isk) proteins to form cardiac I-Ks potassium channel. *Nature*. 384:80–83.
- Sanguinetti, M.C., C. Jiang, M.E. Curran, and M.T. Keating. 1995. A mechanistic link between an inherited and an acquired cardiac arrhythmia: HERG encodes the IKr potassium channel. *Cell*. 81: 299–307.
- Sanguinetti, M.C., and N.K. Jurkiewicz. 1990. Two components of cardiac delayed rectifier K<sup>+</sup> current. Differential sensitivity to block by class III antiarrhythmic agents. *J. Gen. Physiol.* 96:195–215.
- Sanguinetti, M.C., and N.K. Jurkiewicz. 1991. Delayed rectifier outward K<sup>+</sup> current is composed of two currents in guinea pig atrial cells. *Am. J. Physiol.* 260:H393–H399.
- Schulze-Bahr, E., Q. Wang, H. Wedekind, W. Haverkamp, Q. Chen, and Y. Sun. 1997. KCNE1 mutations cause Jervell and Lange-Nielsen syndrome. *Nat. Genet.* 17:267–268.
- Sesti, F., M. Straforini, T.D. Lamb, and V. Torre. 1994. Gating, selectivity and blockage of single channels activated by cyclic GMP in retinal rods of the tiger salamander. *J. Physiol. (Lond.)*. 474: 203–222.
- Shen, K.Z., A. Lagrutta, N.W. Davies, N.B. Standen, J.P. Adelman, and R.A. North. 1994. Tetraethylammonium block of Slowpoke calcium-activated potassium channels expressed in *Xenopus* oocytes: evidence for tetrameric channel formation. *Pflügers Arch.* 426:440–445.
- Shen, Z., and D.C. Marcus. 1998. Divalent cations inhibit Isk/KvLQT1 channels in excised membrane patches of strial marginal cells. *Hearing Res.* 123:157–167.
- Sigworth, F.J., and J. Zhou. 1992. Ion channels. Analysis of nonstationary single-channel currents. *Methods Enzymol.* 207:746–762.
- Splawski, I., M. Tristani-Firouzi, M.H. Lehmann, M.C. Sanguinetti, and M.T. Keating. 1997. Mutations in the hminK gene cause long QT syndrome and suppress IKs function. *Nat. Genet.* 17:338–340.
- Tai, K.-K., K.-W. Wang, and S.A.N. Goldstein. 1997. MinK potassium channels are heteromultimeric complexes. *J. Biol. Chem.* 272:1654–1658.
- Tai, K.K., and S.A.N. Goldstein. 1998. The conduction pore of a cardiac potassium channel. *Nature*. 391:605–608.
- Takumi, T., H. Ohkubo, and S. Nakanishi. 1988. Cloning of a membrane protein that induces a slow voltage-gated potassium current. *Science*. 242:1042–1045.
- Tzounopoulos, T., H.R. Guy, S. Durell, J.P. Adelman, and J. Maylie. 1995. MinK channels form by assembly of at least 14 subunits. *Proc. Natl. Acad. Sci. USA*. 92:9593–9597.
- Tzounopoulos, T., J. Maylie, and J.P. Adelman. 1998. Gating of Isk channels expressed in *Xenopus* oocytes. *Biophys. J.* 74:2299–2305.
- Walsh, K.B., J.P. Arena, W.M. Kwok, L. Freeman, and R.S. Kass. 1991. Delayed-rectifier potassium channel activity in isolated membrane patches of guinea pig ventricular myocytes. *Am. J. Physiol.* 260:H1390–H1393.
- Wang, K.W., and S.A.N. Goldstein. 1995. Subunit composition of minK potassium channels. *Neuron*. 14:1303–1309.
- Wang, Q., M.E. Curran, I. Splawski, T.C. Burn, J.M. Millholland, T.J. VanRaay, J. Shen, K.W. Timothy, G.M. Vincent, T. de Jager, et al. 1996b. Positional cloning of a novel potassium channel gene: KVLQT1 mutations cause cardiac arrhythmias. *Nat. Genet.* 12:17–23.
- Wang, K.-W., K.-K. Tai, and S.A.N. Goldstein. 1996a. MinK residues line a potassium channel pore. *Neuron*. 16:571–577.
- Wollnik, B., B.C. Schroeder, C. Kubisch, H.D. Esperer, P. Wieacker, and T.J. Jentsch. 1997. Pathophysiological mechanisms of dominant and recessive KVLQT1 K<sup>+</sup> channel mutations found in inherited cardiac arrhythmias. *Hum. Mol. Genet.* 6:1943–1949.
- Yang, Y., and F. Sigworth. 1998. Single-channel properties of I<sub>Ks</sub> potassium channels. *J. Gen. Physiol.* 112:665–678.